Volume 1 Issue 1

SURFACE SCIENCE

An International Journal

Full Paper

SSAIJ, 1(1), 2016 [015-026]

Simulation of thermal transport and ablation of thin film copper by fs laser pulse

F.M.Jasim[2], K.I.Mohammed[1], M.I.Azawe[2]*

[1]Department of Physics, College of Science, Kirkuk University, (IRAQ)

[2]Department of Physics, College of Education, Mosul University, (IRAQ)

E-mail : muzahim_935@yahoo.com

ABSTRACT

The nonequilibrium thermal transport for electrons and lattice is described using two-temperature model simulation. The simulation was performed by finite difference time domain provided that dynamical optical and thermophysical properties had been taken into account. The effects of these properties on the electron and lattice temperatures were discussed. It was shown that the peak surface temperature is greater for long pulse duration and the film undergoes a superheated and experiencing a fast cooling compared to the other pulse durations. The ablation depth was found to increase as laser fluence increased. Results show diffusivity, as an electron temperature dependent, a more penetration was occurred resulting in a more ablation per pulse and lower ablation threshold. The dynamic changes of optical properties during laser irradiation, distributions of laser heat density, and electron and lattice temperature of a copper film irradiated by ultrashort-pulsed lasers were investigated, and was found that both the optical properties could drastically decrease during laser irradiation, leading to different laser energy deposition, both in magnitude and spatial distribution. The detailed features of the crater will be discussed.

KEYWORDS

Thermal transport simulation;
Two-temperature model;
Laser materials processing;
Femtosecond laser ablation;
Dynamical optical and thermophysical properties.

INTRODUCTION

Laser pulse of very short duration irradiation to a very small geometrical dimension of a foil, can produce an extreme heat flux. Such an ultrafast heating of the foil can be well described by the so-called two-temperature model (TTM), initial conditions and boundary-valued partial differential equations[28]. Theory of heat transmission based on Fourier's law predicts infinite propagation speed heat disturbances. This law relates heat flux and the temperature gradient. According to this law, heat flux adjusts immediately to the imposed temperature gradient, i.e., there is no relaxation time for the heat flux[22]. During pico- to femtosecond (fs) laser-materials processing, the characteristic times of the heat carriers are comparable to the characteristic energy excitation time[1]. This process has the ability to deposit high density energy at a given place in a very short period of time. Ultrashort pulsed laser is an ideal tool for high-resolution, high-quality micromachining on a wide range of materials[19].

Full Paper

Femtosecond laser has very high peak power, but it causes a limited heat-affected zone in the material because of its ultrashort pulse duration[18]. Two types of the material removal mechanisms are often categorized: thermal ablation and non-thermal ablation. The former includes ultrafast phase changes through melting and vaporization as well as phase explosion if laser fluences are sufficiently high, while the latter is caused by thermal stresses, coulomb explosion, and/or hot electron blast when the laser is operated at fluences slightly exceeding the ablation threshold[44]. The main features of fs pulse laser ablation are; (i) very rapid energy deposition and creation of vapor and plasma phases, (ii) absence of the molten material, and (iii) negligible heat-affected zones[30]. Dynamical investigation of the femtosecond laser ablation using the numerical solution of the theoretical model describing ultrashort high power laser action on metals in the approximation of the hydrodynamic type of TTM with explicit tracking of interphase fronts had been done[49]. Thermophysical and optical properties are the key parameters that govern the two-temperature model solution accuracy. The former, including thermal conductivities, heat capacities and relaxation times of electrons and lattice as well as the electron-phonon coupling factor, were investigated for Ni in a range of temperatures typically realized in femtosecond laser material processing applications, from room temperature up to temperatures of the order of 10^4 K. [27]. Thermophysical properties based on the electron density of state and the effect of thermal excitation of electrons had used with TTM[26]. The latter, including surface reflectivity and absorption coefficient has been paid less attention. In the early time of the numerical TTM study, the thermophysical properties employed are either constant or only adequate for low temperature and the surface reflectivity (R) and optical penetration depth (δ) are often arbitrarily assumed or kept constant[21]. Two-temperature model had been applied to describe the temperature-dependent optical properties of lattice temperature distribution of dielectrics generated by femtosecond lasers[20]. The change of absorptance of copper processed by multi-pulse femtosecond laser had been studied, and it was found that after irradiation, the absorptance of copper had a dramatically increased, meaning that the surface reflectivity was in a big reduction[41]. The threshold fluence for ultra-short single pulse laser ablation is an important parameter and depending on the thermal and dynamical properties of the material[33].

Thermal process following the absorption of laser pulse and the influence of electron-lattice relaxation is the objective of this research, since ion emission would occur as a consequence of such process[1], and the hot electrons could trigger the emission coherent acoustic phonon emission travelling a distance many times larger than the skin depth[25].

In this article,, the mechanism of laser–metal interaction will be thoroughly investigated under the frameworks of the two-temperature model taking into account the thermophysical and optical properties of the copper films as temperature dependent. Numerical simulations will be performed of material ablation by a single laser fs pulse. The numerical results of thermal response and ablation parameters generated by the fs-laser pulse are presented and discussed.

Two-temperature model

In order to write down the equations for electrons and lattice, the following assumptions can be drawn from the theoretical descriptions of the transient temperature response of the copper under the influence of fs laser radiation:

Electron-phonon interaction is the dominant mechanisms of energy transport after the very short laser pulse laser absorption.

The lattice and electrons are described by separate temperatures T_l and T_e, respectively.

The equation for electron temperature can be written as[9]:

$$C_e(T_e).\frac{\partial T_e}{\partial t}=\nabla.(k_e(T_e).\nabla T_e)-G(T_e)\left[T_e-T_l\right]+P(r,t) \quad \textbf{(1)}$$

The equation for the lattice temperature:

$$C_l(T_l).\frac{\partial T_l}{\partial t}=G(T_e)\left[T_e-T_l\right] \quad \textbf{(2)}$$

where C, T, and G are the specific heat capacity, temperature, and electron-phonon coupling, respectively. The subscripts e and l stand for the electron and lattice, respectively. P is the heat deposition rate due to laser source radiation absorption.

k_e is the electron thermal conductivity, and a general expression valid over a wider range of temperatures has to be used[2]:

$$k_e = \chi \frac{\left(\vartheta_e^2 + 0.16\right)^{1.25}\left(\vartheta_e^2 + .44\right)\vartheta_e}{\sqrt{\vartheta_e^2 + 0.092}\left(\vartheta_e^2 + \eta\vartheta_l\right)} \quad (3)$$

where $\vartheta_e = k_B T_e / \varepsilon_F$ and $\vartheta_l = k_B T_l / \varepsilon_F$, k_B is the Boltzmann's constant, ε_F is the Fermi enetgy of copper, and χ coefficient for electronic conductivity.

The electron heat capacity dependence on the electron temperature can be expressed as[3]:

$$C_e(T_e) = \int_{-\infty}^{\infty} \left(\varepsilon - \varepsilon_F\right) \frac{\partial f\left(\varepsilon, \mu, T_e\right)}{\partial T_e} g(\varepsilon) d\varepsilon \quad (4)$$

where $g(\varepsilon)$ is the electron DOS at the energy level ε, μ the chemical potential at T_e and $f\left(\varepsilon, \mu, T_e\right)$ is the Fermi distribution function, defined as[27]:

$$f\left(\varepsilon, \mu, T_e\right) = \left\{ \exp\left[\frac{(\varepsilon - \mu)}{k_B T_e}\right] + 1 \right\}^{-1} \quad (5)$$

The determination of the chemical potential μ, required in Eq. (5), is done through setting the result of the integration of the product of DOS and the Fermi distribution function at T_e overall energy levels to be equal to the total number of valence electrons (9).

The electronic specific heat capacity is taken to be proportional to the electron temperature as[12]:

$$C_e(T_e) = \gamma T_e \quad (6)$$

where γ is the coefficient for electronic heat capacity. The values of the parameters for copper will be given in a table for numerical simulation.

The electron-phonon coupling factor $G(T_e)$ accounting for the thermal excitation of electrons from the energy levels located below the Fermi level can be expressed as[46]:

$$G(T_e) = \frac{\pi \hbar k_B \lambda \left\langle \omega^2 \right\rangle}{g\left(\varepsilon_F\right)} \int_{-\infty}^{\infty} g^2(\varepsilon) \left(-\frac{\partial f}{\partial \varepsilon}\right) d\varepsilon \quad (7)$$

where λ is the electron-phonon coupling constant in the superconductivity theory and $\left\langle \omega^2 \right\rangle$ is the second moment of the phonon spectrum defined by[32].

The laser source $P(r,t)$ can affect both the electron and lattice temperatures and hence the laser heat source has to be characterized properly, i.e., a flat-top laser beam (uniform intensity over the entire laser spot) is considered[9]. Laser in the short pulse regime is a multi-step process; energy is first absorbed in the skin depth by the free electrons and then transported by diffusion and interaction with the atomic lattice, i.e., heating the atoms and breaking the chemical bonds[5].

The following assumption has to be made that the excited electrons are immediately and fully thermalized when the laser pulse is applied[10]. The laser source can be written as[43]:

$$P(x,z,t) = \sqrt{\frac{\beta}{\pi}} \cdot \frac{(1 - R(T_e)) J_O}{t_p \delta} \left[1 + \cos\left(\frac{2x}{L}\pi\right)\right] \cdot \exp\left[-\frac{z}{\delta} - \beta\left(\frac{t - 2t_p}{t_p}\right)^2\right] \quad (8)$$

where J_o is the laser fluence (J/m^2), $R(T_e)$ is the copper surface reflectivity, t_p is the laser pulse duration, $\delta(=\frac{1}{\alpha})$ is the optical penetration depth of photons in copper (where the intensity amplitude is decreased by a factor e), L is the spatial period with $\left(-L/2 \le x \le L/2\right)$ and *z* is the depth coordinate of copper film, and $\beta = 4\ln(2)$ is the normalization factor that describes the temporal Gaussian pulse function[31]. In other words, the laser source is assumed to be cosine function along the surface (along the x-axis) and attenuates exponentially into the copper skin depth (along the z-axis).

The temperature dependencies of the optical characteristics, $\alpha(T_e)$, and $R(T_e)$ were taken from Ref.[30, 31]. The dynamic changes of optical properties α and *R* during laser irradiation, distributions of laser heat density, and electron and lattice temperature of a copper film irradiated by ultrashort-pulsed lasers were investigated, and was found that both the optical properties could drastically decrease during laser irradiation, leading to different laser

energy deposition, both in magnitude and spatial distribution, in the heated material[36, 44].

Lasing is assumed to start at t=0 and ends at t=4t_p, and the laser energy outside this period of time is neglected since it is too small to significantly affect the electron temperature[9]. This condition satisfies that the laser pulse is entirely absorbed at the beginning of the pulse by electron gas near the metal surface and the energy is distributed at fs scale (pulse duration) in the entire thin film by collision to the atomic lattice through electron-phonon coupling.

The initial values TTM are as follows. The initial conditions for both electrons and phonons are:

$$T_e\left(z,-2t_p\right)=T_l\left(z,-2t_p\right)=T_o \quad \textbf{(9)}$$

with T_o is the initial temperature. Here we assume that the thermal wave does not reach the remote boundary during the calculation time[29].

Ablation depth

The ablation depth can be expressed as[13, 37, 13]:

$$L \cong \delta.\ln\left(\frac{F}{F_{th}^{\delta}}\right) \text{ for low } F_{th} \text{ (skin depth)} \quad \textbf{(10)}$$

$$L \cong l\ln\left(\frac{F}{F_{th}^{l}}\right) \text{ for high } F_{th}$$

(electron heat conduction) **(11)**

The two ablation regimes in laser ablation are the multi-photon (skin depth) and the electron diffusion (thermal) regimes, respectively. These come out of the Arrhenius-type evaporation equations, and describe the ablation process by for high-intensity ablation[15].

For low incident fluences, the skin depth (defined above as δ) defines the effective depth of absorption, because the density of hot electrons is relatively low and the laser pulse energy is mainly deposited in the shallow region which is the penetration depth. In the higher laser fluences, the contribution of electronic heat conduction becomes more significant, and the electron thermal diffusion length (defined as $l \approx \sqrt{D\tau_a}$) dominates and increases the ablation rate over that of the skin depth[15].

Numerical results

The numerical analysis was performed for copper film using the two-temperature model, and simulation results for thermal transport for copper heated by femtosecond laser pulse will be presented by finite- difference time domain (FDTD). This method is essentially grid-based differential time domain numerical modeling method. The method is discretized and implemented in Matlab. The results will show some differences than the published results in the temperature distribution and in the electron temperature. First of all, the increment in time of stable and convergent solution was carried out and adjusted until a high resolution of the model was obtained.

The simulation results for ultrafast laser interaction with a thin copper film (thin film thickness was 200 nm and the substrate was silica) were initially at 300 K will be presented. The electron and lattice temperature at the front surface are presented in Figure (1) against time with laser fluence of 0.8 J/cm^2, wavelength 800 nm[25], with a spot size of 20 μm in diameter keeping the spot size much larger than the sample thickness, and pulse duration 80 fs. The results simulated by the TTM with dynamic optical and thermophysical properties.

The simulation was carried out at laser intensity ($I=10^{13}$ *W/cm^2*), but really the onset of the plasma regime takes place[5]. This value should be large enough to trigger the formation of plasma on the surface, and the onset of plasma in front of the target will be affecting all optical and thermal properties of the target and of laser-matter interaction[5].

The different times of the peak temperatures of electron and lattice are obvious, and the lattice had a lag time of 0.2 ps to reach its maximum temperature. It is important to emphasize that the calculated temperatures T_e & T_l were influenced from the laser matter interaction mechanism and needs around 2.0 ps to come to balance. Also the curve indicates the thermal electron role is insignificant above 2.0 ps. The simulation underlying that with increasing pulse duration longer than t_p 2.1 ps, the TTM suggests nonequilibrium thermal transport for electrons and lattice no longer exists.

When the ionization is completed, the plasma formed in the skin-layer of the target has a free-electron density comparable to the ion density of about

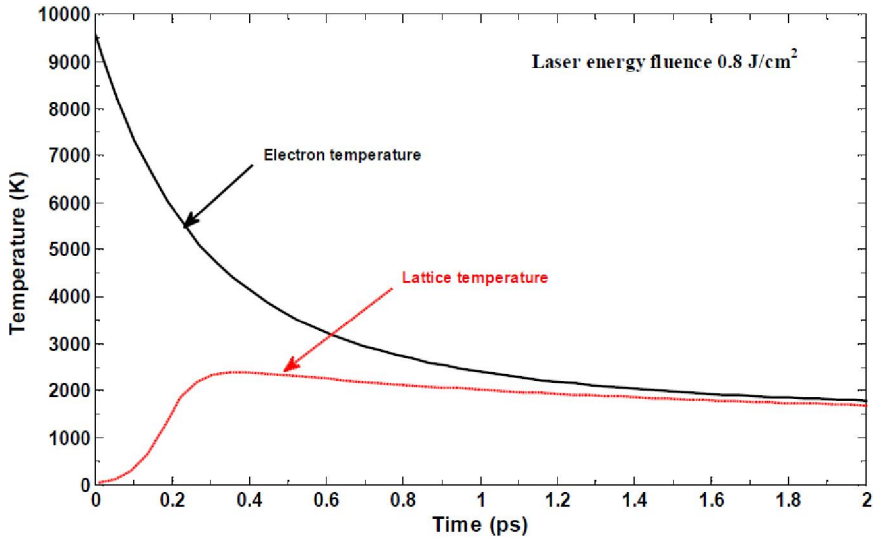

Figure 1 : Time evolution of electron and lattice temperatures at the front surface of copper when irradiated by 0.8 J/cm^2 with pulse duration of 80 fs, and wavelength 800 nm

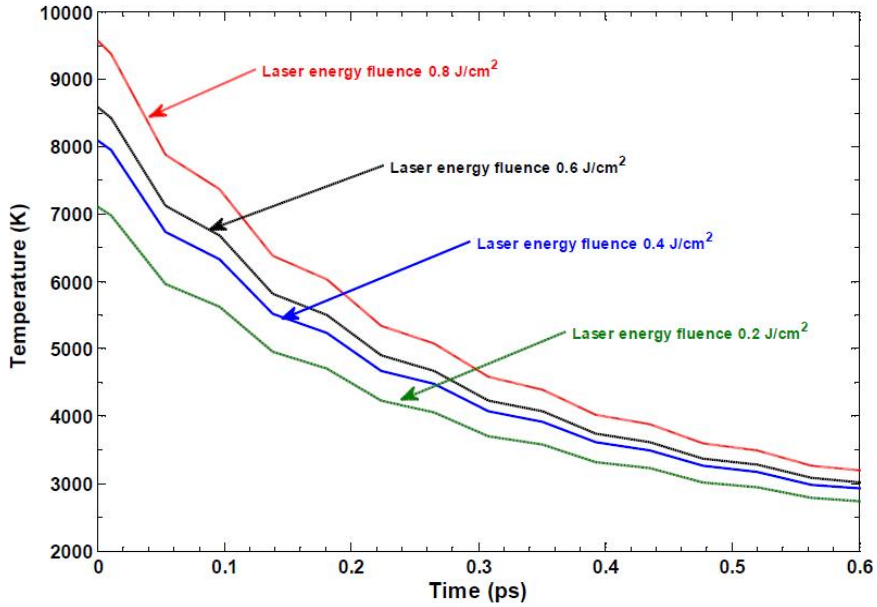

Figure 2 : Time-dependent electron temperature for different laser fluence and constant pulse duration of 80 fs

10^{23} cm^{-3}, and in order to meet the ablation conditions the average electron energy should increase up to the Fermi energy, i.e. up to several eV[14, 8].

The time-dependent of electron temperature, as can be seen from the previous figure is an exponential decay, but this decay was found to be in form shown in Figure (2) for different laser fluence as 0.8, 0.6, 0.4, and 0.2 J/cm^2. The time scale was expanded in order to show this behavior and the electron temperature started to decrease with undulation due to electron-lattice heat exchange by thermal waves. Thermal waves propagate through the medium with a speed of $v_{th} = \sqrt{D_e(T_e)/\tau_e}$, depending on the electron relaxation time τ_e , and when this time increases, the speed v_{th} will be decreased. $D_e(T_e)$ is the electron thermal diffusivity. Also this effect could be interpreted due surface plasmon since copper has a real part of dielectric constant smaller than (-1) and to compare the incubational behavior of this metal with other metal whether surface plasmon play an important role or not[16].

The plasma electron temperature-density crossed gradients may modify the beam transport in a time scale of a few picoseconds but in shorter time scales, this effect can be neglected. The plasma electrons have been heated up to the Fermi temperature by fs

laser pulse duration in the thin film, and consequently the electrical resistivity in this film goes from the cold solid-liquid phase to the hot plasma one and decreases with the temperature. The consequence is that it creates electrical resistivity gradients in the target which tend to hollow the beam generates an electric field which tends to eject the plasma electrons out of the beam volume in order to equilibrate the total charge in a timescale of the order of the inverse of the plasma electron-ion collision frequency[39].

Figure (3) shows the influence of laser pulse duration on the spatial distribution of the laser heat source. The surface temperatures are all follow an exponential decay. The dynamical optical and thermophysical properties had been taken into account and the 1nm step for simulation was carried out. The peak temperature is greater for long pulse duration and the film undergoes a superheated and experiencing a fast cooling compared to the other pulse durations. Thermal diffusion length, on the other hand, was increased for a longer pulse duration as a square law dependence and can be observed when (1/e) of surface temperature was estimated. Laser fluence was taken as low as 0.2 J/cm^2 since for high laser fluence, thermal diffusion dominates and increases the ablation rate over the skin depth. This will conclude that the ablation rate decreased as the pulse length was increased[16]. It was found that the damage threshold increased with pulse duration[6], which agrees with the previous research on fs laser ablation of Cu and Al films and fs laser ablation of fused silica[23, 35]. Damage threshold is a characteristic dependent on the wavelength, pulse width and type of material; it is ideally defined as the laser fluence at which irreversible damage occurs in the material by removing a monolayer of material[16].

The figure shows the surface temperature profiles along the direction normal to the copper thin film surface after the absorption of different laser pulse widths. Clearly, the spatial surface temperature distributions are very different in all these cases. When the laser pulse was 120 fs the surface temperature had a steeper spatial distribution. In other words, it deceases fast with the diffusion depth. The higher electron temperature within a narrower spatial range means that most of the absorbed laser energy is confined within a very small volume because of weaker electron diffusion. In contrast, for the case of low laser pulse duration, the spatial surface temperature distribution becomes relatively flatter, indicating that the absorbed laser energy spreads widely in a larger volume and the electron diffusion becomes stronger.

To investigate the influence of laser pulse dura-

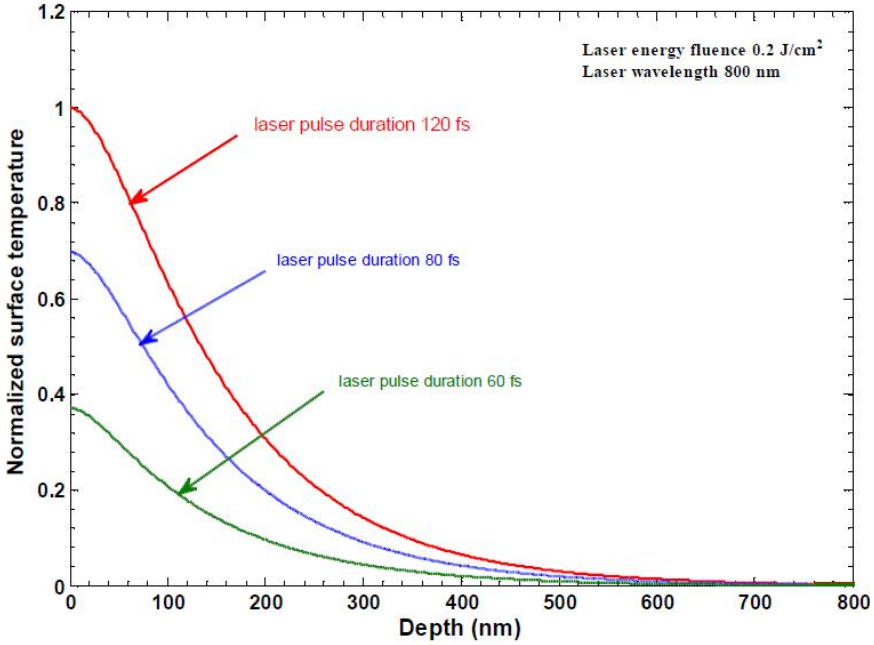

Figure 3 : Normalized surface temperature varrying with pulse duration. Normaliztion of temperature was taken with respect to the temperature at 120 fs laser pulse. Laser fluence was 0.2 J/cm^2

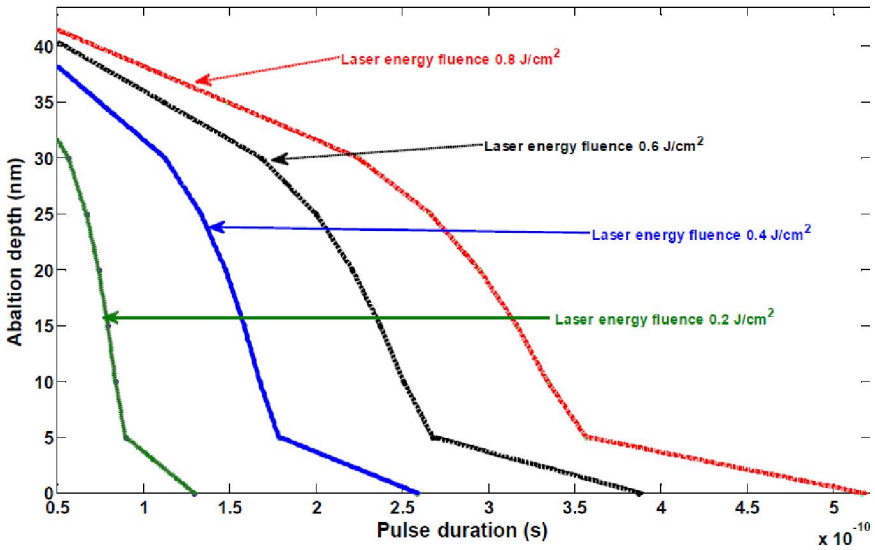

Figure 4 : Shows the ablation depth as a function of single laser pulse duration, for different laser fluence

tion and laser fluence on the ablation depth, the simulation results are shown in Figure (4). The depth removed per incident fluence could be a relevant parameter to estimate the ablation efficiency at fixed pulse duration. The ablation depth was found to increase as laser pulse and laser fluence increase. Hence, it is worth mentioning that it is important to point out that the higher laser fluence leads to a strong ablation, which is much larger than the fluence that generated a gentle ablation located in the vicinity of central pulse incidence.

The nonlinear dependence of ablation depth with fluence is attributed to more efficient multi-photon ionization at higher peak intensities and plasma density increases with the laser intensity rising[14]. The multiphoton absorption associated with the high intensity of fs pulse is responsible for bond breaking and sub- sequent emission of electrons and ions[6]. Experimentally, it was confirmed that ablation depth increased with increasing both the laser fluence and laser pulse duration but with fixed repetition rate, and explained due heat accumulation[7]. At low fluence, the pulse heating of the material is not enough to reach a temperature high enough in order to vaporize the material; hence pulse duration should be increased.

Nolte et al. (1997) pointed out that when the laser energy deposition is determined by the optical penetration depth (first ablation regime) no trace of molten material can be observed, but at a higher fluences (second ablation regime), a thin layer of molten material appears. Increasing pulse duration reduces the effective energy penetration depth and increases the threshold fluence. Both effects can be explained by hydrodynamic plasma expansion during the laser pulse, plasma shielding of the laser radiation, and increased heat-conduction losses[33].

The effects of dynamical properties on the ablation depth will be studied in the following figure. Electron temperature dependence on the dynamical properties was found to be a crucial upon ablation depth. It should be emphasized that, the ablation threshold fluence corresponds to the removal of an ablated volume equal to zero[24]. Ablation threshold fluence was calculated to be 0.68 J/cm^2 when the electron temperature dependent was taken into account, while a threshold value of 1.92 J/cm^2 when simulation was carried out as the electron temperature independent.

Figure (5), the ablation depth dependence on the laser fluence for 120 fs laser pulse, shows two different logarithmic dependences that can be explained when the electron thermal diffusion length (defined as) taken to be electron temperature dependence, and can be written as, accordingly:

$$l(T_e) \approx \sqrt{D_e(T_e)\tau_a} \qquad (12)$$

Hence, diffusivity can play an important role in ablation process. When simulations were carried out for diffusivity as electron temperature dependent, a more penetration was occurred resulting in a more ablation per pulse and lower ablation threshold. Another feature that can be observed from the figure was the nonlinearity in the behavior of the curve at

Full Paper

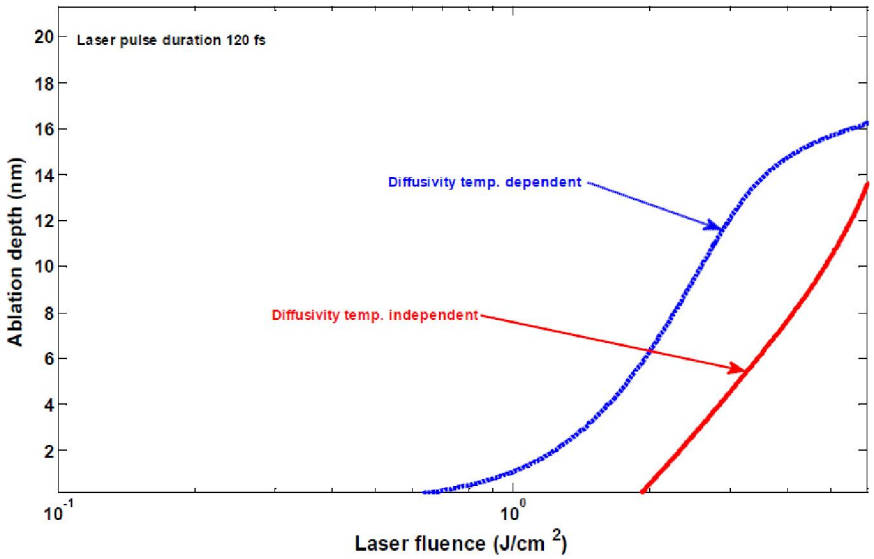

Figure 5 : Illustrates the effects of diffusivity on the abaltion threshold and ablation depth of copper thin film with incident fluence for 120 fs

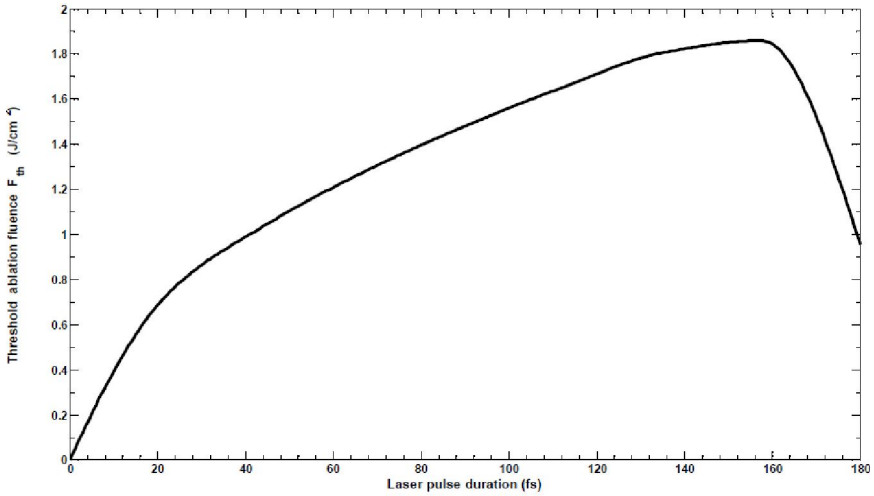

Figure 6 : Represents the simulation results of threshold ablation fluence versus laser pulse duration when diffusivity was taken as electron temperature dependent. The laser fluence was 0.6 J/cm^2

higher laser fluence because no consideration was taking into account for the relaxation time in both heat flux and temperature gradient, i.e., a dual phase lag should be considered at high laser fluence.

The influence of laser pulse duration on the threshold ablation fluence in the thermal diffusion regime, the simulation results are shown in Figure (6).

The laser fluence was during the regime characterized by the high-energy penetration depth, and the increase of the threshold ablation fluence with laser pulse duration due to the increase of thermal diffusion length. The behavior is nonlinear because of the logarithm relation between the thermal diffusion length and threshold ablation fluence. The maximum threshold ablation fluence was found as 1.86 J/cm^2 at laser pulse duration of 160 fs and in addition to this, a sharp decrease in the threshold ablation fluence was occurred after this pulse duration. In the simulation, the diffusivity was taken to be dependent on the electron temperature. This drop in the threshold ablation fluence can be related to the electron-lattice coupling at higher laser pulse duration giving high value for the surface temperature as illustrated in Figure (3), with high pulse duration surface temperature was increased. Balling and Schou used lattice temperature in their calculation to determine the threshold ablation and its dependence on the laser pulse duration[4], with a behavior similar to our result except the sharp decrease.

The evolution of electron temperature is obviously follows the signature of the laser pulse duration and as the laser pulse increased; electron temperature becomes lower than the electron temperature without the diffusivity was taken into account. On the other hand, threshold ablation fluence was decreased when laser pulse duration was increased can be attributed to the reduction of laser irradiance as laser fluence was kept constant resulting in a much decreased ablation efficiency, and especially when considering the crater depth evolution versus fluence.

The peak value (optimum) in the threshold ablation fluence can be explained as the fluence for which there is a significant and ultrafast nonlinear ionization by the very leading edge of the pulse, up to the critical density, giving rise to a highly efficient linear absorption of the intensity peak[11]. This is attributed to the development of the plasma formed in a thin surface layer of the copper, becoming gradually overcritical at the beam center and reflecting or screening the late part of the beam. In other words, the plasma formed acts as an optical ultrafast shutter with the switching (closing) time being shorter and more efficient when the pulse duration decreased[38].

The simulation on the ablation crater created by focused single laser pulse on the surface of copper is shown in Figure (7) plotted as a function of the pixel number. Laser fluence was 0.6 J/cm2 and pulse duration of 80 fs. These values were taken from the previous simulation to assure it is near the optimum values and close to the ablation threshold with higher laser irradiance. The detailed features of the crater will be discussed on basis of simulation carried out with TTM and taking into account the dynamical optical and thermophysical properties. The hole represents the characteristic of high-temperature melting inside the ablation region. The distinct ring around the hole with a black color, which is almost the size of the laser beam waist, is the result of a heat-affected zone on the surface of copper. The next zones of lower temperature expand dramatically on the surface and with nonuniform temperature distribution. The asymmetry in the expanded rings can be attributed to the laser beam characteristics and laser-copper interaction. In the simulation a Gaussian beam was considered. The profile around the crater reveals a nonuniform progression in material removal, which relates to known imperfections in the intensity distribution of the laser beam employed and also related to the complex nature of the laser surface interaction[34]. Xin-yu et al. (2009) studied the spatially nonuniform heat distribution for Cu and Ag. Due to the very short time scales involved in the ablation with femtosecond laser pulses, the ablation process can be considered as a direct solid-vapor transition. Laser energy is absorbed by the electrons much faster than it can be transferred to the lattice, and since the lattice does not heat appreciably during the pulse, there is no need to track the flow of energy into the lattice to account for thermal and mechanical stresses[48].

The parameters of copper used in the simulation are given in TABLE 1. The thermophysical proper-

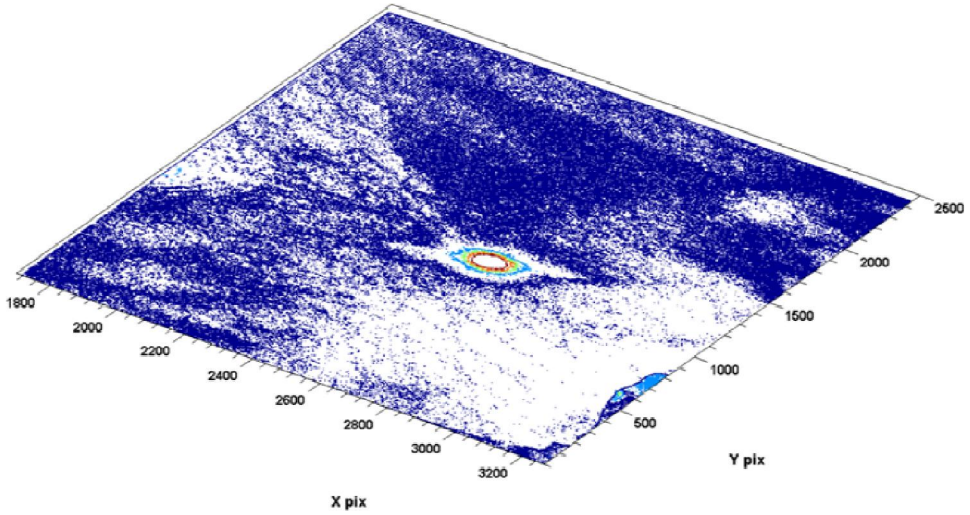

Figure 7 : Surface features of Cu induced by a single 80 fs laser pulse duration and laser fluence of 0.6 J/cm^2 . The crater is surrounded by rings showing the temperature spatial distribution nonuniformally

Full Paper

TABLE 1 : Parameters of copper used in the simulation

Properties	Value
Lattice room temperature T_l (K)	300
Thermal conductivity (W/m.K)	$407.88-0.0272\times T_l - 2.658\times10^{-5}\times T_l^2 - 3.0\times10^{-9}\times T_l^3$
Molar weight, M (kg/kmol)	63.546
Boiling temperature (K)	2835
Melting temperature (K)	1357
Femi energy (eV)	7.04
Density (kg/m^3)	8.94×10^3
Specific heat (J/kg. K)	$313.75+0.324\times T_l - 2.687\times10^{-4}\times T_l^2 + 1.2568\times10^{-7}\times T_l^3$
Thermal expansion (25°C) (μm/m.K)	16.5
Fermi velocity (m/s)	1.57×10^6
Ionization (eV)	7.7264

ties used in the calculations were taken from Ref.[36]. Electron relaxation time of copper at room temperature was taken as 25 fs[44].

CONCLUSIONS

Numerical simulation results for thermal transport of copper heated by femtosecond single laser pulse were studied. The simulation was performed using TTM by FDTD when the dynamical optical and thermophysical properties had been included in the simulation. Time evolution of electron temperature and surface temperature as a function of penetration depth were studied. It was found that electron temperature after reaching its maximum value decreased with undulation. The lattice reached its maximum temperature in 300 fs. The undulation in electron temperature decrease was explained due to surface plasmons in copper. Ablation parameters were investigated in the simulation in terms of ablation depth and threshold ablation fluence. Dynamical optical and thermophysical properties were found to have an impact on the ablation depth. The results also showed that diffusivity had pronounced effects on the ablation threshold and ablation depth of copper film. The laser pulse duration was found to have a crucial effect on the threshold ablation fluence. Crater formation on the surface of copper was found to have a spatially nonuniform temperature distribution. The ablation yield as a function of fluence and taking into account both the pulse duration and its propagation inside the material can influence the crater topography profile. Crater depth and the diameter of the ablated crater have been found to be laser parameters dependent, especially, the laser fluence and single pulse duration, and dynamical optical and thermophysical properties.

ACKNOWLEDGMENTS

The work presented here was performed in the University of Mosul, College of Education and with as a part of Research and Activities of the staff members of the University. The authors thank Prof. D. Batani for fruitful discussions concerning the numerical aspects of the paper.

REFERENCES

[1] S.Amoruso, X.Wang, C.Altucci, C.de Lisio, M.Armenante, R.Bruzzese, R.Velotta; Thermal and nonthermal ion emission during high-fluence femtosecond laser ablation of metallic targets, Appl.Phys.Lett., **77**, 3728 **(2000)**.

[2] S.I.Anisimov, B.Rethfeld; On the theory of ultrashort laser pulse interaction with a metal, Proc.Nonresonant Laser-Matter Interaction (NLMI-9), St.Petersburg, Russia, SPIE, Bellingham, Washington, DC, **3093**, 192–203 **(1997)**.

[3] N.W.Ashcroft, N.D.Mermin; Solid state physics, Holt, Rinehart and Winston, New York, **(1976)**.

[4] P.Balling, J.Schou; Femtosecond-laser ablation dynamics of dielectrics: basics and applications for thin films, Rep.Prog.Phys., **76**, 036502 **(2013)**.

[5] D.Batani; Short-pulse laser ablation of materials at

high intensities: Influence of plasma effects, Laser and Particle Beams, **28**, 235 **(2010)**.

[6] Q.Bian, X.Yu, B.Zhao, Z.Chang, S.Lei; Femtosecond laser ablation of indium tin-oxide narrow grooves for thin film solar cells, Opt.Laser Tech., **45**, 395 **(2013)**.

[7] F.Brygo, Ch.Dutouquet, F.Le Guern, R.Oltra, A.Semerok, J.M.Weulersse; Laser fluence, Repetition rate and pulse duration effects on paint ablation, Appl.Surf.Sci., **252**, 2131 **(2006)**.

[8] Byskov J.Nielsen, J.M.Savolainen, M.S.Christensen, P.Balling; Ultra-short pulse laser ablation of metals: Threshold fluence, Incubation coefficient and ablation rates, Appl.Phys.A, **92**, 576 **(2010)**.

[9] J.K.Chen, J.E.Beraun, L.E.Grimes, D.Y.Tzou; Modeling of femtosecond laser-induced non-equilibrium deformation in metal films, Int.J.Solids and Structures, **39**, 3199 **(2002)**.

[10] J.K.Chen, D.Y.Tzou, J.E.Beraun; A semiclassical two-temperature model for ultrafast laser heating.Int.J.Heat and Mass Transfer, **49**, 307 **(2006)**.

[11] B.Chimier, O.Utéza, N.Sanner, M.Sentis, T.Itina, P.Lassonde, F.L´egar´e, F.Vidal, J.C.Kieffer; Damage and ablation thresholds of fused-silica in femtosecond regime, Phys.Rev.B, **84**, 094104 **(2011)**.

[12] I.H.Chowdhury, X.Xu; Heat transfer in femtosecond laser processing of metal, Num.Heat Trans., Part A, **44**, 219 **(2003)**.

[13] P.J.Ding, Q.C.Liu, X.Lu, X.L.Liu, S.H.Sun, Z.Y.Liu, B.T.Hu, Y.H.Li; Hydrodynamic simulation of silicon ablation by ultrashort laser irradiation, Nucl.Instr.Meth.B, **286**, 40 **(2012)**.

[14] E.G.Gamaly, A.V.Rode, Luther B.Davies, V.T.Tikhonchuk; Ablation of solids by femtosecond lasers: Ablation mechanism and ablation thresholds for metals and dielectrics, Phys.Plasmas, **9**, 949 **(2002)**.

[15] P.Gonzales, R.Bernath, J.Duncan, T.lmstead, M.Richardson; Femtosecond ablation scaling for different materials, Proc.SPIE, **5458**, 265 **(2004)**.

[16] M.Hashida, A.Semerok, O.Gobert, G.Petite, Y.Izava, J.F.Wagner; Ablation threshold dependence on pulse duration for copper, Appl.Surf.Sci., **862**, 197-198 **(2002)**.

[17] A.Hu, Y.Zhou, W.W.Duley; Femtosecond laser-induced nanowelding: fundamentals and applications, Open Sur.Sci.J., **3**, 42 **(2011)**.

[18] H.Huang, A.Hu, P.Peng, W.W.Duley, Y.Zho; Femtosecond laser-induced microwelding of silver and copper, Appl.Opt., **52(6)**, 1211 **(2013)**.

[19] J.Huang, Y.Zhang, J.K.Chen; Ultrafast solid–liquid–vapor phase change of a gold film induced by pico- to femtosecond lasers, Appl.Phys.A, **95**, 643 **(2009)**.

[20] L.Jiang, H.L.Tsai; Prediction of crater shape in femtosecond laser ablation of dielectrics, J.Phys.D: Applied Physics, **37**, 1492 **(2004)**.

[21] M.Kaganov, I.M.Lifshitz, L.V.Tanatarov; Relaxation between electrons and crystalline lattices, Sov.Phys.JETP., **4**, 173 **(1957)**.

[22] V.V.Kulish, V.B.Novozhilov; An integral equation for the dual-lag model of heat transfer, J.Heat Trans., **126**, 805 **(2004)**.

[23] Le Harzic, R.D.Breitling, M.Weikert, S.Sommer, C.Fohl, S.Valette; Pulse width and energy in fluence on laser micromachining of metals in arrange of 100 fs to 5ps. Appl.Surf.Sci., **249(1–4)**, 322 **(2005)**.

[24] M.Lebugle, N.Sanner, O.Utéza, M.Sentis; Guidelines for efficient direct ablation of dielectrics with single femtosecond pulses, Appl.Phys.A, **114**, 129 **(2014)**.

[25] M.Lejman, V.Shalagatskyi, O.Koalenko, T.Pezeril, V.V.Temnov, P.Ruello; Ultrafast optical detection of coherent acoustic phonons emission driven by superdiffusive hot electrons, J.Opt.Soc.Am., **31**, 282 **(2104)**.

[26] Z.Lin, L.V.Zhigilei; Electron-phonon coupling and electron heat capacity of metals under conditions of strong electron-phonon nonequilibrium, Phys.Rev.B, **77**, 075133 **(2008)**.

[27] Z.Lin, L.V.Zhigilei; Temperature dependences of the electron–phonon coupling, electron heat capacity and thermal conductivity in Ni under femtosecond laser irradiation, Appl.Surf.Sci., **253**, 6295 **(2007)**.

[28] E.Majchrzak, J.Poteralska; Numerical analysis of short-pulse laser interaction with thin metal film, Archives of Foundry Engineering, **10(4)**, 123 **(2014)**.

[29] W.Marine, N.M.Bulgakova, L.Patrone, I.Ozerov; Insight into electronic mechanisms of nanosecond-laser ablation of silicon, J.Appl.Phys., 094902 **(2008)**.

[30] A.V.Mazhukin, V.I.Mazhukin, M.M.Demin; Modeling of femtosecond ablation of aluminum film with single laser pulses, Appl.Surf.Sci., **257**, 5443 **(2011)**.

[31] V.I.Mazhukin, A.V.Mazhukin, O.N.Koroleva; Optical properties of electron Fermi-gas of metals at arbitrary temperature and frequency, Laser Phys., **19(5)**, 1179 **(2009)**.

[32] W.L.McMillan; Transition temperature of strong-coupled superconductors, Phys.Rev., **167**, 331 **(1968)**.

Full Paper

[33] S.Nolte, C.Momma, H.Jacobs, A.Tünnermann, B.N.Chichkov, B.Wellegehausen, H.Welling; Ablation of metals by ultrashort laser pulses, J.Opt.Soc.Am.B, **14(10)**, 2716 **(1997)**.

[34] D.G.Papazoglou, V.Papadakis, D.Anglos; In situ interferometric depth and topography monitoring in LIBS elemental profiling of multi-layer structures, J.Anal.At.Spectrom., **19**, 483 **(2004)**.

[35] M.D.Perry, B.C.Stuart, P.S.M.D.Banks, Feit, V.Yanovsky, A.M.Rubenchik; Ultrashort-pulse laser machining of dielectric materials, J.Appl.Phys., **85(9)**, 6803 **(1999)**.

[36] Y.Ren, J.K.Chen, Y.Zhang; Properties and thermal response of copper films induced by ultrashort-pulsed lasers, J.Appl.Phys., **110**, 113102 **(2011)**.

[37] D.E.Roberts, Du A.Plessis, L.R.Both; Femtosecond laser ablation of silver foil with single and double pulses, Appl.Surf.Sci., **256(6)**, 1784 **(2009)**.

[38] J.Roth, A.Krauß, J.Lotze, H.R.Trebin; Simulation of laser ablation in aluminum: The effectivity of double pulses, Appl.Phys.A, **117**, 2207 **(2014)**.

[39] M.Touati, J.L.Feugeas, Ph.Nicolaï, J.J.Santos, L.Gremillet, V.T.Tikhonchuk; A reduced model for relativistic electron beam transport in solids and dense plasmas, New J.Phys., **16**, 073714 **(2014)**.

[40] D.Y.Tzou, J.K.Chen, J.E.Beraun; Hot-electron blast induced by ultrashort-pulsed lasers in layered media, Inter.J.Heat and Mass Trans., **45**, 3369 **(2002)**.

[41] A.Y.Vorobyev, C.Guo; Change in absorptance of metals following multi-pulse femtosecond laser ablation, J.Phys.: Conf.Series, **59**, 579 **(2007)**.

[42] G.X.Wang, V.Prasad; Microscale heat and mass transfer and nonequilibrium phase change in rapid solidification, Mater.Sci.Eng.A, **292(2)**, 142 **(2000)**.

[43] J.Wang, C.Guo; Numerical study of ultrafast dynamics of femtosecond laser-induced periodic surface structure formation of noble metals, J.Appl.Phys., **102**, 053522 **(2007)**.

[44] S.Y.Wang, Y.Ren, C.W.Cheng, J.K.Chen, D.Y.Tzou; Micromachining of copper by femtosecond laser pulses, Appl.Surf.Sci., **265**, 302 **(2013)**.

[45] S.Y.Wang, Y.Ren, C.W.Cheng, J.K.Chen, D.Y.Tzou; Micromachining of copper by femtosecond laser pulses, Appl.Surf.Sci., **265**, 302 **(2013)**.

[46] X.Y.Wang, D.M.Riffe, Y.S.Lee, M.C.Downe; Time-resolved electron temperature measurement in a highly-excited gold target using femtosecond thermionic emission, Phys.Rev.b, **50**, 8016 **(1994)**.

[47] Xin T.Yu, Duan Z.ming, M.Feng, Zhi L.hua, Y.Di, Xiao Z.Zhong; Theoretical and experimental study of energy transportation and accumulation in femtosecond laser ablation on metals, Trans.Nonferrous Met.Soc.China, **19**, 1645 **(2009)**.

[48] Y.L.Yao, H.Chen, W.Zhang; Thermal aspects in laser material removal, Proc.NSF workshop on research needs in thermal aspects of material removal processes, Oklahoma State University, Stillwater, OK, June 10-12 **(2003)**.

[49] J.Zhang, Y.Zhao, X.Zhu; Theoretical studies of ultrafast ablation of metal targets dominated by phase explosion, Appl.Phys.A, **89**, 571 **(2007)**.